LSG1-VAP binding promotes 60S Large Ribosomal Subunit Assembly

Claire Goul, Serim Yang, Sara Bonini, Nikolay Aleksashin, Rose Citron, Hijai Regina Shin, Jamie Cate, Dominic Winter, Roberto Zoncu

https://doi.org/10.1590/SciELOPreprints.14782

Submitted on: 2026-01-07
Posted on: 2026-03-04 (version 1)
(YYYY-MM-DD)

LSG1-VAP binding promotes 60S Large Ribosomal Subunit Assembly

Claire Goul
University of California at Berkeley, Berkeley, CA, USA.
ORCID: https://orcid.org/0000-0002-6556-9631

Serim Yang
University of California at Berkeley, Berkeley, CA, USA.
ORCID: https://orcid.org/0009-0001-1787-2636

Sara Bonini
University of Duisburg-Essen, Essen, Germany.
ORCID: https://orcid.org/0000-0001-8293-2546

Nikolay A Aleksashin
University of California at Berkeley, Berkeley, CA, USA.
ORCID: https://orcid.org/0000-0002-3403-7587

Y. Rose Citron
University of California at Berkeley, Berkeley, CA, USA.
ORCID: https://orcid.org/0000-0001-6090-7243

Hijai Regina Shin
University of Texas Southwestern Medical Center, Dallas, TX, USA.
ORCID: https://orcid.org/0000-0001-5642-4441

Jamie HD Cate
University of California at Berkeley, Berkeley, CA, USA.
ORCID: https://orcid.org/0000-0001-5965-7902

Dominic Winter
University of Duisburg-Essen, Essen, Germany.
ORCID: https://orcid.org/0000-0001-6788-6641

Roberto Zoncu
University of California at Berkeley, Berkeley, CA, USA.
ORCID: https://orcid.org/0000-0003-1611-1891

Abstract
Ribosome biogenesis requires coordinated assembly of ribosomal subunits in the nucleus and cytoplasm. The GTPase LSG1 facilitates cytoplasmic maturation of the large 60S subunit by releasing the adaptor NMD3, enabling its nuclear recycling. Here we identify LSG1 as an interactor of the endoplasmic reticulum membrane proteins VAPA and VAPB through two functional FFAT motifs. Mutation of conserved aromatic residues within these motifs abolishes VAP binding and disrupts LSG1 localization to the ER. Split-proximity labeling reveals that LSG1-VAP sites are enriched for NMD3, the upstream GTPase GTPBP4, and ribosomal proteins. Importantly, loss of VAP binding impairs NMD3 nuclear recycling and causes accumulation of free ribosomal subunits, indicating defective 80S assembly. Preliminary evidence suggests phosphorylation of Thr320 within the second FFAT motif enhances VAP binding, potentially linking LSG1 activity to cellular metabolic states. These findings establish a critical role for ER-localized LSG1 in coordinating late-stage ribosome maturation.

Keywords:
ribosome biogenesis, ribosome assembly

Introduction

Ribosomes are essential for protein synthesis and cell growth. A single mammalian cell contains on the order of 10×10^6 ribosomes, each assembled from four distinct ribosomal RNAs and roughly 80 proteins. The synthesis and assembly of these components into mature ribosomes is highly regulated and tightly coordinated to ensure proper assembly. In eukaryotes, ribosome biogenesis begins in the nucleolus, where precursor large (60S) and small (40S) subunits are formed. These pre-ribosomal particles transit the nucleoplasm, are exported through the nuclear pore complex (NPC), and undergo final maturation steps in the cytoplasm. Assembly proceeds through a series of checkpoints—ATP- or GTP-dependent events coordinated by numerous protein chaperones and assembly factors that associate and dissociate in a defined sequence. Although many individual factors have been identified, and the human 60S structures during assembly recently solved[1], ribosome assembly has primarily been studied in budding yeast (*S. cerevisiae*), and how the successive stages of ribosome assembly are integrated to meet the translational demands and increased complexity of human cells remains to be clarified[2].

In yeast, export of the pre-60S subunit through the NPC requires the adaptor protein Nmd3, which recruits the export karyopherin Xpo1/Crm1[3]. Once in the cytoplasm, the GTPase Lsg1 triggers the release of Nmd3, completing 60S maturation[4,5,6]. Mammals encode an orthologous GTPase, LSG1, but its regulation and precise function are less well characterized. Given that the guanine nucleotide–bound state of many regulatory GTPases (e.g., KRas4B, Rheb, RagA/B) is rapidly tuned by nutrient availability and other environmental inputs, the energetically demanding process of ribosome biogenesis may likewise be coupled to cellular metabolism through LSG1.

The endoplasmic reticulum (ER) is a major site of protein translation, particularly for secreted and membrane proteins, and also serves as a signaling hub through membrane contact sites (MCS) with the plasma membrane, Golgi apparatus, mitochondria, and lysosomes. The integral ER proteins VAPA and VAPB (collectively VAPs) are key organizers of these contacts. Their N-terminal major sperm protein (MSP) domain specifically binds FFAT motifs—short acidic sequences typically containing “two phenylalanines in an acidic tract” (consensus EFFDAxE) or related variants [7,8].

Bioinformatic analysis of protein sequences and protein–protein interaction datasets revealed two candidate FFAT motifs within LSG1. Immunoprecipitation, fluorescence polarization, and live imaging experiments demonstrated that LSG1 binds VAPA and VAPB through these FFAT motifs and that this interaction is required for LSG1 localization to the ER. We demonstrate that LSG1 binds VAPA and VAPB through these FFAT motifs and that this

interaction is required for nuclear recycling of NMD3 and assembly of the large ribosomal subunit. Future studies are needed to determine whether the LSG1-VAP interaction is regulated under specific cellular conditions and to further clarify the consequences for ribosome assembly and global translation.

Results

LSG1 binds VAPs via two FFAT motifs

To identify novel interactors of the ER membrane proteins VAPA and VAPB, we mined the BioGRID protein–protein interaction database[9]. Among 57 proteins predicted to bind both VAPA and VAPB, many were known lipid-transfer or membrane-contact–site factors (e.g., members of the ORP family). One candidate, however, stood out: LSG1, a ribosome assembly factor whose potential interaction with VAPs had not been previously characterized.

LSG1 contains two predicted FFAT motifs (a.a. 306-312 and 317-322; **Fig. 1A**). Indeed, immunoprecipitations of $VAPA^{WT}$ or $VAPB^{WT}$ pulled down endogenous LSG1, but VAP mutants defective in FFAT motifs ($VAPA^{K94D,M96D}$ and $VAPB^{K87D,M89D}$) failed to recover LSG1 (**Fig. 1B**). Consistently, wild-type LSG1 pulled down endogenous VAPs, but mutation of the aromatic residues in FFAT#1 and FFAT#2 abolished binding (**Fig. 1C)**. As with other canonical FFAT motifs, the aromatic residues were critical, although acidic residues also contributed, as evidenced by residual binding of endogenous VAPs to $LSG1^{D322A,E329A}$ (**Fig. 1C**).

Competition assays further supported a direct LSG1-VAP interaction. Addition of synthetic peptides corresponding to LSG1 FFAT#1, LSG1 FFAT#2, or the well-characterized FFAT of OSBP to cell lysates prior to VAPA or VAPB immunoprecipitation displaced endogenous interactors, whereas a scrambled control peptide had no effect. (**Fig. 1D, Fig. 1E**). Likewise, addition of these peptides prior to LSG1 immunoprecipitation disrupted recovery of endogenous VAPs (**Fig. 1F**). Direct binding was further validated by fluorescence polarization experiments, in which unlabeled LSG1 FFAT#1 and FFAT #2 peptides outcompeted binding of FAM-labeled OSBP FFAT, with FFAT#2 exhibiting weaker binding compared to FFAT#1 (**Fig. 1G**).

Consistent with a robust ER association, live imaging of GFP-tagged $LSG1^{WT}$ revealed a reticular, ER-like distribution. In contrast, VAPA/B double knockdown or mutation of both FFAT motifs resulted in diffuse cytosolic localization (**Fig. 1H**). Together, these complementary approaches demonstrate that LSG1 interacts with both VAPA and VAPB through its two FFAT motifs, with the conserved aromatic residues playing an essential role in binding.

LSG1-VAP binding promotes NMD3 recycling and 60S assembly

To uncover the functional consequences of the LSG1-VAP interaction, we first sought to determine the local-neighborhood of proteins at LSG1-VAP sites. We performed split-proximity biotinylation (split-TurboID[10]) between wild-type LSG1 and VAP (TiDC-$LSG1^{WT}$ + TiDN-$VAPB^{WT}$) and compared the resulting biotinylated proteome with that obtained from two controls-TiDC-$OSBP^{WT}$-TiDN-$VAPB^{WT}$, which marks canonical OSBP-VAP sites, and TiDC-$LSG1^{Y307A,W318A}$-TiDN-$VAPB^{WT}$, expected to have minimal biotinylation. Normalization of the wild-type LSG1-VAPA TurboID to the $LSG1^{Y307A,W318A}$-$VAPB^{WT}$ revealed robust enrichment of VAPA, multiple components of the ER translocon (3 enriched out of 4 detected), and ribosomal proteins from both the large (5 enriched out of 43 detected) and small subunits (6 enriched out of 33 detected)(**Fig. 2A**). Among the most strikingly enriched factors was NMD3, the chaperone needed for the nuclear export of pre-60S particles. The 60S GTPase GTPBP4, which acts in a checkpoint upstream of LSG1 in the large subunit maturation, was also highly enriched.

To reveal whether the neighborhood of LSG1-VAP sites was distinct from that of OSBP-VAP sites, we directly compared the LSG1-VAPB and OSBP-VAPB interactomes (**Fig. 2B**). NMD3 again emerged as the most enriched biotinylated protein other than LSG1 itself, with GTPBP4 and numerous ribosomal proteins and proteosome subunits also overrepresented.

These data suggest that the LSG1-VAP sites are functionally distinct from OSBP-VAP sites and enriched for proteins involved in late-stage ribosome biogenesis.

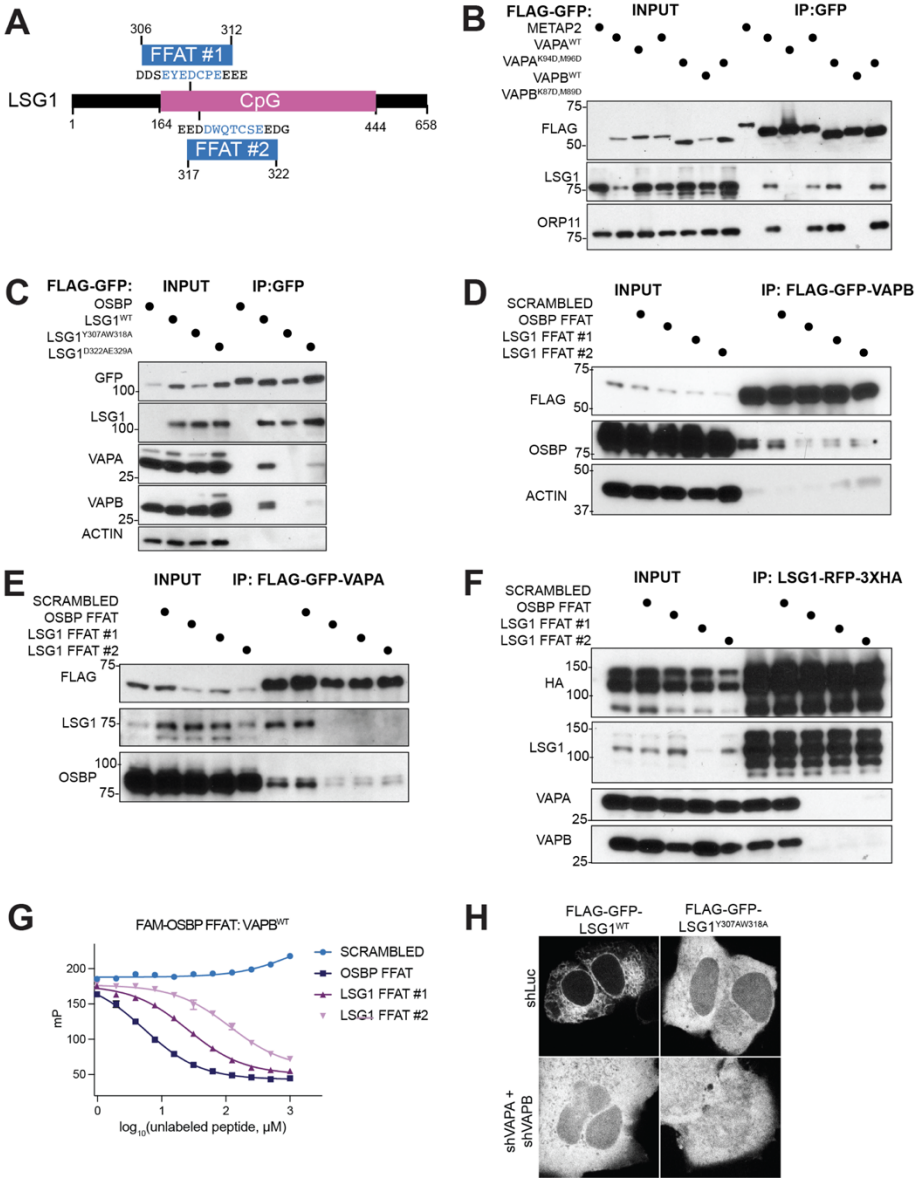

Figure 1. LSG1 binds to VAPs via aromatic residues in its FFAT motifs.
(A) Overview of the domain organization of LSG1 (CpG, Circularly permutated-type Guanine nucleotide binding domain, pink; FFAT #1 and FFAT #2, blue)
(B) Western blot of immunoprecipitated METAP2, and wild-type or FFAT-binding mutant VAPA and VAPB.
(C) Western blot of immunoprecipitated OSBP, and wild-type, aromatic FFAT mutant, or acidic FFAT mutant LSG1.
(D) Western blot of immunoprecipitated VAPB from lysates preincubated with indicated FFAT peptides.
(E) Western blot of immunoprecipitated VAPA from lysates preincubated with indicated FFAT peptides.
(F) Western blot of immunoprecipitated LSG1 from lysates preincubated with indicated FFAT peptides.

(G) Fluorescence polarization (mP: millipolarization) curves resulting from FAM-OSBP bound to purified VAPB protein treated with the indicated unlabeled FFAT peptides.
(H) Confocal microscopy of HEK293T cells stably expressing FLAG-GFP-LSG1^{WT} or FLAG-GFP-LSG1^{Y307A,W318A} following transduction with shRNAs targeting Luciferase (Luc) as a control or VAPA and VAPB.

Because yeast Lsg1 is required for the release and nuclear recycling of Nmd3[3], the presence of NMD3 as a top interactor prompted us to test a similar role for human LSG1. Using cells with endogenously tagged mNeonGreen-NMD3, we observed that NMD3 normally localizes throughout the cell with marked enrichment in nucleoli, consistent with prior reports. Depletion of LSG1, or of the upstream assembly factor C1orf109 as a positive control[11], caused a striking exclusion of NMD3 from the nucleus (**Fig. 2C**). Re-expression of LSG1^{WT} restored the nuclear and nucleolar distribution of NMD3, whereas re-expression of VAP-binding-deficient mutant LSG1^{Y307A,W318A}failed to do so (**Fig. 2C, D**). Notably, NMD3 exclusion from the nucleus in LSG1-knockdown cells reconstituted with LSG1^{Y307A,W318A} was indistinguishable from that of LSG1 knockdown, indicating that LSG1 binding to VAP is required for the recycling of NMD3 back to the nucleus.

We next asked whether impaired NMD3 recycling corresponds to a defect in ribosomal large-subunit assembly. Polysome profiling of cells depleted for C1orf109, LSG1, or LSG1 followed by reconstitution with LSG1^{Y307A,W318A} revealed an accumulation of free 40S and 60S subunits relative to 80S, indicating a defect in ribosome assembly (**Fig. 2E**).

Together, these findings demonstrate that the LSG1-VAP interaction is functionally important in human cells. By recruiting LSG1, VAP facilitates NMD3 recycling to the nucleus and ensures efficient maturation of the 60S ribosomal subunit.

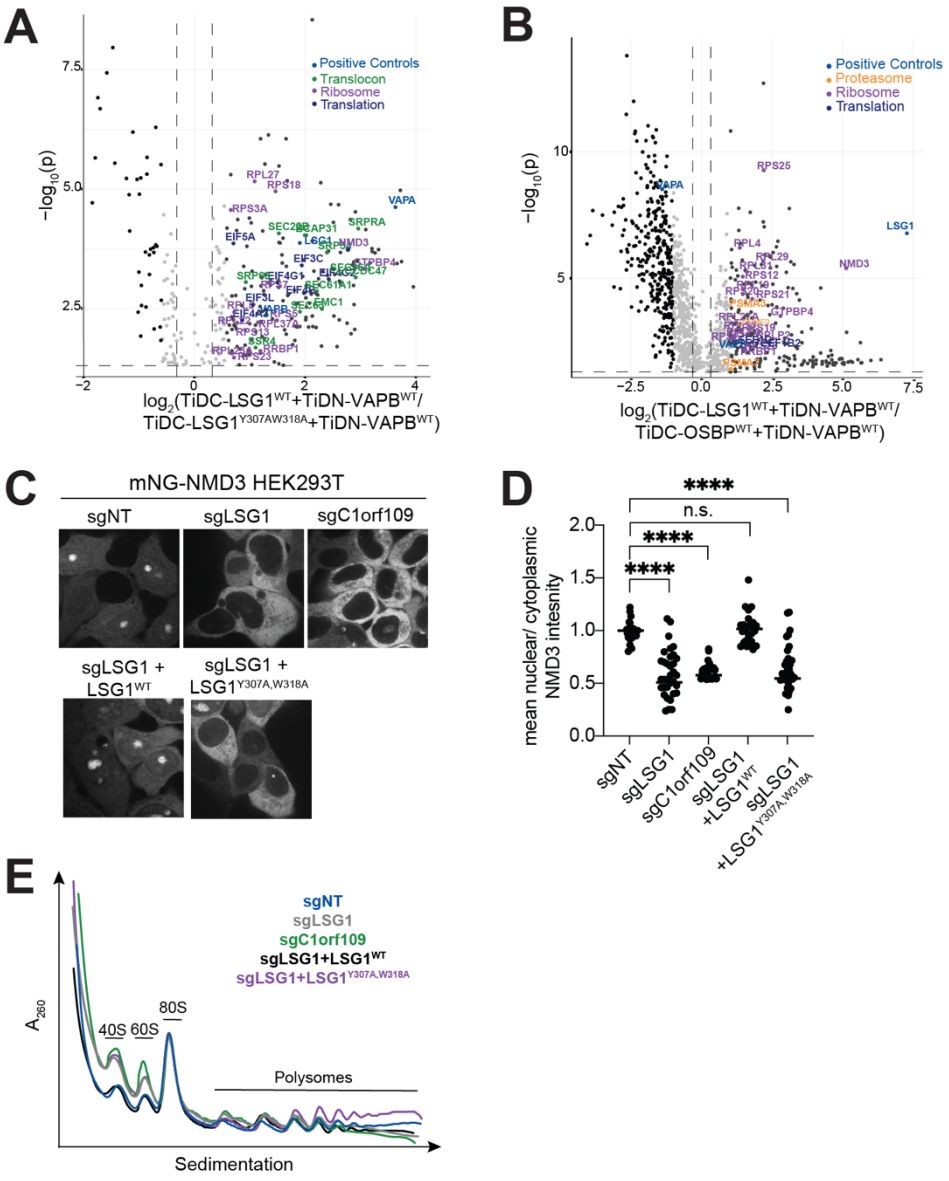

Figure 2 LSG1-VAP interaction promotes NMD3 nuclear recycling and ribosome assembly.
(A) Split TurboID (TiD) of wild-type LSG1 and wild-type VAPB (TiDC-LSG1^{WT} + TiDN-VAPB^{WT}), normalized to split-TiD of FFAT mutant LSG1 and wild-type VAPB (TiDC-LSG1^{Y307A,W318A} + TiDN-VAPB^{WT}). Black and colored points are statistically significant ($p < .05$, $\log_2FC > 1.5$).
(B) Split TurboID (TiD) of wild-type LSG1 and wild-type VAPB (TiDC-LSG1^{WT} + TiDN-VAPB^{WT}), normalized to split-TiD of OSBP and wild-type VAPB (TiDC-OSBP + TiDN-VAPB^{WT}).
(C) Live imaging of endogenously tagged mNeonGreen (mNG)-NMD3 HEK293T cells. Cells were imaged following transduction with single guide RNAs (sgRNAs) (nontargeting: NT) and reconstitution with 3XHA-LSG1^{WT} or 3XHA-LSG1^{Y307A,W318A}.
(D) Quantification of mean intensity of NMD3 in the nucleus relative to the cytoplasm in mNG-NMD3 HEK293T cells.
(E) Polysome profiles of HEK293T cells following transduction with sgRNAs and reconstitution with 3XHA-LSG1^{WT} or 3XHA-LSG1^{Y307A,W318A}. A260 (Absorbance at 260 nm).
Comparison of groups carried out by one-way ANOVA (C). ****$p<0.0001$, n.s. not significant.

FFAT motif phosphorylation enhances LSG1 ER localization

Phosphorylation of Ser/Thr residues in FFAT motifs enhances binding to the VAP MSP domain[12]. We identified two candidate phosphorylation sites in FFAT#2 (Thr 320, Ser, 322) and assessed the consequences of phosphorylation on the VAP-LSG1 interaction. Fluorescence polarization experiments showed that Thr 320- phosphorylated FFAT#2 peptide bound recombinant VAPB with a higher affinity than the corresponding non-phosphorylated peptide (**Fig. 3A**).

Consistent with the in vitro binding, GFP-tagged phospho-null LSG1 (LSG1^{T320A}) no longer exhibited a reticular, ER-like distribution and instead was diffusely distributed throughout the cytoplasm, while phospho-mimetic mutants (LSG1^{T320D}, LSG1^{T320E}) displayed an intermediate phenotype, consistent with a failure to fully recapitulate phosphorylation with these amino acid substitutions (**Fig. 3B**). Co-expression of GFP-tagged LSG1^{T320A} with VAPA^{WT}-mCherry failed to restore the reticular localization observed with GFP-LSG1^{WT} (**Fig. 3C, Fig. 3D**). Phospho-mimetic mutants again showed a partial co-localization with VAPA (**Fig. 3D**), suggesting that aspartate/glutamate substitutions may not fully recapitulate phosphorylation in this context.

Immunoprecipitation experiments revealed reduced binding of phospho-null mutant LSG1 to both VAPA and VAPB (**Fig. 3E**). Together, these findings suggest that phosphorylation of Thr 320 within FFAT#2 would promote LSG1-VAP association in cells, while additional validation is needed to determine the consequences of Ser 322 phosphorylation. Future work is also needed to confirm phosphorylation of these sites in cells, identify the responsible kinase, and determine how this phosphorylation is regulated.

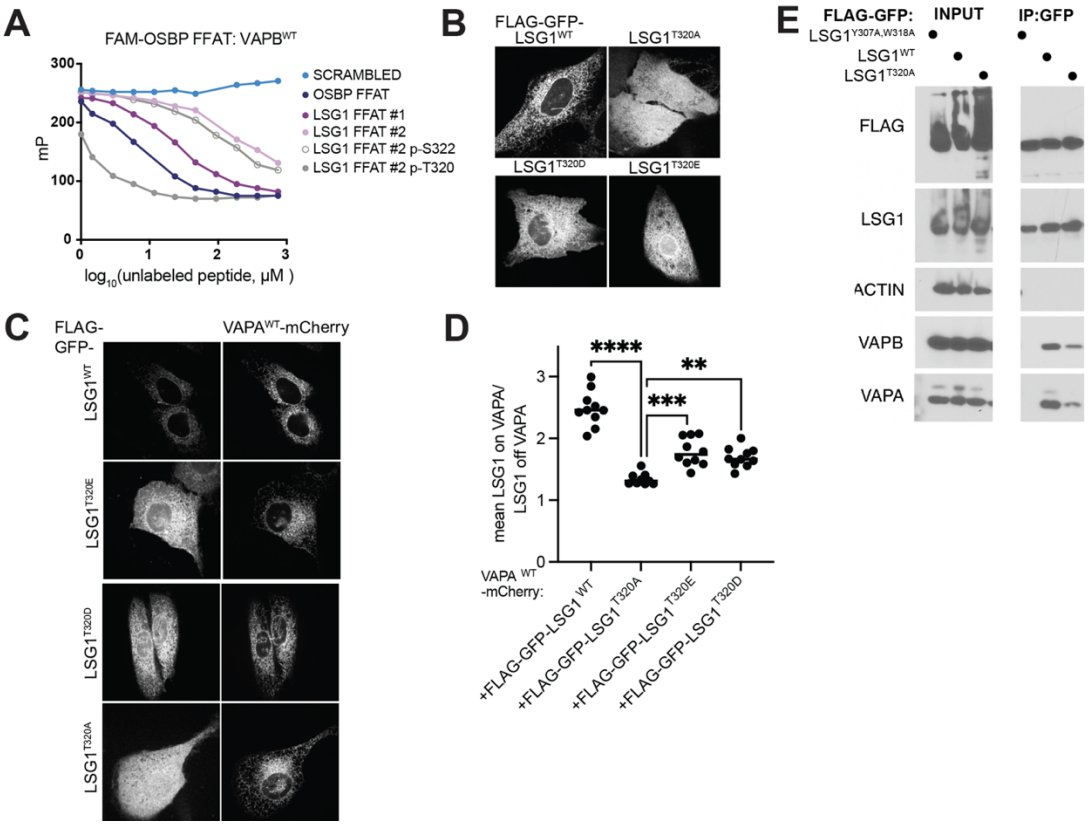

Figure 3. Characterization of putative phosphorylation of LSG1 FFAT #2 motif.
(A) Fluorescence polarization (mP: millipolarization) curves resulting from FAM-OSBP bound to purified VAPB protein treated with the indicated unlabeled FFAT peptides.

(B) Confocal microscopy of HEK293T cells stably expressing FLAG-GFP-LSG1 wild-type, phospho-mimetic mutants (LSG1^{T320D}, LSG1^{T320E}), or phospho-null mutant (LSG1^{T320A}).
(C) Confocal microscopy of HEK293T cells stably expressing FLAG-GFP-LSG1 wild-type, phospho-mimetic mutants (LSG1^{T320D}, LSG1^{T320E}), or phospho-null mutant (LSG1^{T320A}) co-transfected with VAPA-mCherry.
(D) Quantification of colocalization ratio between LSG1 and VAPA (mean intensity of LSG1 on VAPA/ mean intensity of LSG1 off VAPA) in cells co-expressing LSG1 constructs and VAPA-mCherry.
Comparison of groups carried out by one-way ANOVA (D). ****p<0.0001, ***, p<0.001, **p<.01, n.s. not significant.

Discussion

Our findings demonstrate that the ribosome assembly GTPase LSG1 localizes to the ER through direct binding to VAPA/B. The LSG1-VAP interaction promotes 60S assembly, establishing a new functional link between ER membrane contact sites and ribosome biogenesis. LSG1 contains two FFAT motifs that engage the VAP major sperm protein (MSP) domains and are essential for localization of LSG1 to the ER. Mutation of the conserved aromatic residues within these motifs abolished VAP binding and resulted in diffuse cytosolic distribution of LSG1. Split-TurboID proximity labeling showed that wild-type LSG1 strongly enriches NMD3, GTPBP4, multiple ER-translocon components, and ribosomal proteins, suggesting that LSG1 operates near late 60S maturation factors. Loss of VAP binding through FFAT mutation impaired nuclear recycling of NMD3 and caused an accumulation of free ribosomal subunits, indicating a defect in 80S assembly.

During the course of this work, an independent study confirmed that LSG1 binds VAP proteins[13]. This independent study supports the conclusion that LSG1 is a bona fide VAP interactor, but reported that deletion of residues 292–324, encompassing the FFAT motifs, did not disrupt NMD3 recycling. In contrast, the data presented here demonstrate a requirement for VAP binding in NMD3 recycling. Several technical distinctions may explain the discrepancy. The published study relied on immunofluorescence, whereas the present work used live imaging of endogenously tagged NMD3. In addition, present experiments used targeted point mutations of the conserved aromatic residues that specifically disrupt FFAT–MSP interactions.

Percentile Rank	Site	Gene Name	Site Percentile	Location
1	S322	FAM20C	99.57	ER, Golgi, Secreted
2	S322	BRAF	99.24	Cytoplasm, Nucleus, Cell membrane
3	S322	PDK4	98.7	Mitochondria
4	S322	CDC7	98.41	Nucleus
5	S322	GRK5	97.86	Cytoplasm, Nucleus, Cell membrane
1	T320	ALPK1	99.57	Nucleus
2	T320	GRK5	99.39	Cytoplasm, Nucleus, Cell membrane
3	T320	CSNK1G3	98.86	Cytoplasm
4	T320	STK39	98.82	Cytoplasm, Nucleus
5	T320	GRK6	98.76	Membrane

Table 1. Top Predicted Kinases for FFAT residues (CST Phosphosite[14]).

A separate recent report demonstrated that deletion of LSG1 alters the translation of a subset of proteins[15]. The current findings raise the possibility that these translational changes may

depend in part on the VAP-bound pool of LSG1. Future work comparing global translation in cells expressing either wild-type LSG1 or FFAT-mutant LSG1 will help distinguish effects of total LSG1 loss from those requiring VAP binding.

Our work suggests that phosphorylation of the FFAT motifs may regulate the LSG1-VAP interaction. Fluorescence-polarization experiments showed that phosphorylation of Thr 320 within FFAT#2 increases binding to VAPB, with additional future work needed to also assess potential Ser 322 phosphorylation in FFAT #2. Kinase prediction databases (Table 1) identified several candidate kinases for these FFATs. Notably, the top predicted kinase for Ser 322 is FAM20C, which phosphorylates secretory proteins and is activated during ER stress[16]. Given that LSG1 depletion alters the translation of secretory proteins[15], it is tempting to speculate that FAM20C-mediated phosphorylation of LSG1 could provide a mechanism to modulate ribosome assembly under conditions that demand altered synthesis of secretory or membrane proteins. Testing whether FAM20C or other predicted kinases phosphorylate LSG1 FFAT residues in cells, and determining the regulatory mechanism of this phosphorylation, represent important next steps.

Our findings support a model in which ER-localized LSG1-VAP complexes serve as hubs for late 60S maturation. Key outstanding questions include: (1) Which kinase(s) phosphorylate LSG1 FFAT motifs, and under what conditions? (2) Does VAP binding affect LSG1 GTPase activity? (3) How does VAP binding facilitate NMD3 release? Future studies addressing these questions will provide valuable insight into the mechanisms governing ribosome assembly in human cells.

Methods

Microscopy

Confocal microscopy was performed on a spinning-disk Nikon Ti-E inverted microscope (Nikon Instruments) with Andor Zyla-4.5 cMOS camera (Andor Technology) using iQ3 acquisition software (Andor Technology). All images were taken with a 60× oil objective. Colocalization analysis was performed by importing raw, unprocessed, non-overlapping images to FIJI v.2.1.0/1.53c. Images of individual channels were thresholded independently to exclude background and converted to binary mask. Colocalization between VAP and LSG1 was determined using the “AND” function of the image calculator.

Protein purification

Human VAPB (6XHIS- TEV-VAPB) was expressed in *Escherichia coli* BL21 cells. Bacteria were grown in Luria broth (LB) medium until OD600 ≈ 0.5, induced with 1 mM isopropylthiogalactoside (IPTG), at 18°C for 18 hr. Cell pellets from 1 L of culture were frozen in LN2, and subsequently resuspended in lysis buffer (10% glycerol, 40 mM Tris pH 8.0, 500 mM NaCl, 10 mM imidazole, 0.5 mM TCEP, protease inhibitor tablet) followed by lysis with a microfluidizer. Lysates were cleared by ultracentrifugation at 24,000 *g* for 30 min at 4°C (Beckman, Brea, CA, USA, Ti45 rotor). Cleared supernatants were applied to Ni-NTA resin (Qiagen, 30230) pre-washed in lysis buffer and incubated with rotation at 4°C for 30 minutes, and the mixture was applied to a gravity column. Following washes with 15 bead volumes of lysis buffer, 6XHIS-TEV-VAPB was rapidly eluted in 4 bead volumes of lysis buffer containing 300 mM imidazole. Elution was evaluated by Coomassie staining, flash frozen in liquid nitrogen, and stored at -80°C.

Plasmids and cloning

Human codon-optimized truncated 6XHIS-TEV-VAPB was cloned into the pET28A. Human codon-optimized LSG1 cDNAs (ordered from IDT) constructs were cloned into pLJM1-FLAG-GFP, pLVX-3XHA, pLJM1-HA-FRB*-TiDC, or pLJM1-RFP-3XHA vectors. Human VAPB was cloned into pLJM1-TiDN-V5-FKBP. All other VAPA and VAPB constructs were previously generated in the lab. sgRNAs were cloned into pLentiCRISPRv2 (sgLSG1: CACACAAGTGAACTCAATGAG, sgC1orf109: CATCGTCCTGGACAAGCTAG).

Peptide binding and fluorescence polarization

A binding curve of FAM-OSBP peptide (DEDDENEFFDAPEIITMP; 50 nM final) with recombinant VAPB was generated by incubating FAM-OSBP peptide with serially two-fold diluted recombinant VAPB (starting at 30 μM), in triplicate. Fluorescence polarization of FAM-peptide was measured on a Tecan Spark Multimode Microplate reader. Recombinant VAPB (0.75 μM final) was incubated with FAM-OSBP peptide (12.5 nM final) for 30 minutes, followed by incubation with 3 mM or serially two-fold diluted unlabeled OSBP FFAT peptide, LSG1 FFAT #1 peptide (TDEDDSEYEDCPEEEEDD), LSG1 FFAT #2 peptide (PEEEEDDWQTCSEEDGPK), LSG1 phospho-Thr peptide (PEEEEDDWQ[pT]CSEEDGPK), LSG1 phospho-Ser peptide (PEEEEDDWQTC[pS]EEDGPK), or scrambled peptide (GADWPMEMRGQANADAGA) in

triplicate for 15 minutes, followed by fluorescence polarization measurement. All peptides were ordered from GenScript. Curves were plotted in Prism v10.2.0 (GraphPad).

Mammalian cell culture

HEK293T cells and their derivatives were cultured in DMEM base media with 10% fetal bovine serum supplemented with 2 mM glutamine, penicillin, and streptomycin. All cell lines were maintained at 37°C and 5% CO2.

Lentivirus production and infection

Lentiviruses were made by co-transfecting pLJM1, pLVX, or pLentiCRISPR constructs with psPAX2 and pMD2G packaging plasmids into HEK293T cells using PEI transfection reagent. Viral supernatant was collected 48-72 h post-transfection and filtered using 0.45 µm syringe filter. The virus was then concentrated using Lenti-X concentrator (Clontech 631231) according to manufacturer's protocol and stored at -80°C. For lentivirus infection, target cells were seeded in 6 well plates and infected the following day with lentivirus and 10 µg/ml polybrene (Millipore TR-1003-G). After 24 hrs, virus was removed, and cells were changed into fresh media containing either Puromycin (1 µg/mL) or Hygromycin B (200 µg/mL) for selection. Experiments on sgRNA transduced cells were performed 6-8 days post transduction. Rescue experiments were conducted by infecting sgRNA transduced cells at day 4 post selection with rescue virus, followed by selection (day 4- day 7), and experiments were performed at day 7.

Proximity biotinylation experiments

HEK293T cells were grown in were cultured in DMEM base media with 10% dialyzed fetal bovine serum supplemented with 2 mM glutamine, penicillin, and streptomycin (DMEM + dFBS) for at least 3 days prior to experiments. Four 15 cm plates per condition were treated for 30 minutes with 50 µM biotin. Following labeling, cells were washed three times in PBS, and chased in DMEM + dFBS for 3 hours. Cell pellets were snap frozen in LN2 and shipped to Dominic Winter's laboratory for downstream analysis. Cell pellets were thawed on ice and resuspended in four pellet volumes of lysis buffer (1% SDS in 50 mM HEPES, pH 7.5) prior to boiling for 5 minutes at 95 °C and pelleting at 13,000 rpm for 10 minutes at room temperature. Streptavidin beads (180 uL slurry for one confluent 15 cm plate, GE17-5113-01) were washed 3 times in IP buffer (0.5% SDS in 50 mM HEPES, pH 7.5), and lysate was added to beads and immunoprecipitated with rotation overnight at 4°C. The following morning, beads were pelleted at 800xg for 1 minute at room temperature, and washes in indicated buffers were carried out sequentially at room temperature (RIPA buffer buffer (50 mM Tris-HCl pH 8, 150 mM NaCl, 0.1 % SDS, 0.5% Sodium Deoxycholate, 1% Triton-X-100, 1x Roche Complete protease inhibitor), 1M KCl, 0.1 M Na_2CO3, 2M Urea in 10mM Tris-HCl pH 8, RIPA buffer, 2 washes in 0.1 M TEAB pH 8, 2M Urea in 0.1 M TEAB pH 8, 2 washes in 0.1 M TEAB pH 8). Proteins were digested on the bead using sequencing grade trypsin and MS analyses carried out using nanoLC-MSMS on UltiMate 3000 RSLCnano system coupled to an Orbitrap Fusion Lumos mass spectrometer as described[17] elsewhere.

Polysome profiling

Sucrose gradients were prepared by underlaying 6 mLs of 50% sucrose solution (50% sucrose, 100 µg/mL cycloheximide, 0.5 mM DTT, 20 mM HEPES-KOH, 100 mM KCl, 5 mM $MgCl_2$) to 6 mLs of 10% sucrose solution (10% sucrose, 100 µg/mL cycloheximide, 0.5 mM DTT, 20 mM HEPES-KOH, 100 mM KCl, 5 mM $MgCl_2$) into centrifuge tubes (Seton, 7030), run on a gradient forming machine, and stored at 4°C while cell samples were prepared. HEK293T cells in 15 cm plates (50% confluent, ~ 10^7 cells) were treated with 100 µg/mL (final) cycloheximide (Sigma, 01810) for 5 minutes. Plates were washed in 5 mL ice cold DPBS (Gibco, 14190-144) supplemented with 100 µg/mL cycloheximide and pelleted at 1500xg for 3 minutes. Cell pellets were lysed in lysis buffer (10mM HEPES-KOH pH 7.4, 10 mM KCl, 1.5 mM $MgCl_2$, 0.5 mM DTT,

1% Triton-X-100, 100 µg/mL cycloheximide) by incubation for 10 minutes on ice, followed by passage 15 times through a 26 G needle using a 1 mL syringe (BD PrecisionGlide Needle, 305111). Lysate was pelleted at 15000 g for 5 minutes, and supernatant A260 was measured. 50-100 pmol of ribosomes were layered onto each gradient, and gradients were spun in SW41 rotor at 37,000 rpm for 2 hours at 4°C prior to fractionation.

Immunoprecipitations

For immunoprecipitations cells were rinsed once with PBS and lysed by rotation for 15 minutes at 4 °C in pS6K buffer (10 mM Na-PPi, 10 mM Na-Beta-glycerophosphate, 40 mM HEPES, 4 mM EDTA, 1% Triton). Lysates were pelleted for 10 minutes at 13,000 g, and supernatant was added to GFP-Trap Agarose (Chromotek, gta) or HA magnetic beads (Pierce, 88836) and immunoprecipitated at 4°C for 1 hour. Following immunoprecipitation, beads were washed 3 times in pS6K buffer and eluted in 5X SDS Sample Buffer (235 MM Tris, 10% SDS, 25% Glycerol, 25% BME, bromophenol blue) by boiling for 5 minutes at 95°C. Immunoprecipitated proteins were resolved by SDS-page and analyzed by immunoblotting.

Statistical analysis

Statistical analyses were performed using unpaired two-tailed Student's *t* tests for comparisons of two groups, one-way analysis of variance (ANOVA) or two-way ANOVA for group comparisons using Prism v10.2.0 (GraphPad). Details of each statistical test are given in the legend accompanying each figure. Curve-fitting for enzyme kinetics and other statistical analyses for peptide binding and polarization experiments are detailed in the appropriate methods.

Authors' contributions statment

C.G. and R.Z. designed the study. Y.R.C., C.G., S.Y., S.B., and H.R.S. performed experiments. C.G., S.Y., H.R.S, and S.Y. analyzed data. J.H.D.C., N.A.A., D.W., and R.Z. supervised the research. C.G. wrote the manuscript with input from all authors.

Conflict of interest statement

The authors declare no competing interests.

Research data availability statement

The entire dataset supporting the results of this study was published in the article itself.

Funding

National Institutes of Health grant 1R35GM149302 (R.Z.); Ara Parseghian Medical Research Foundation grant (R.Z.), a Cancer Research Coordinating Committee predoctoral fellowship (C.G.)

Acknowledgements

Thank you to Jeremy Thorner, Arlen Johnson, Putrl Sujita, and Jordan Ngo for helpful discussions and insightful advice.

References

1. Liang, X. *et al.* Structural snapshots of human pre-60S ribosomal particles before and after nuclear export. *Nat Commun* **11**, 3542 (2020).
2. Klinge, S. & Woolford, J. L. Ribosome assembly coming into focus. *Nat Rev Mol Cell Biol* **20**, 116–131 (2019).
3. Trotta, C. R., Lund, E., Kahan, L., Johnson, A. W. & Dahlberg, J. E. Coordinated nuclear export of 60S ribosomal subunits and NMD3 in vertebrates. *EMBO J* **22**, 2841–2851 (2003).
4. Hedges, J., West, M. & Johnson, A. W. Release of the export adapter, Nmd3p, from the 60S ribosomal subunit requires Rpl10p and the cytoplasmic GTPase Lsg1p. *EMBO J* **24**, 567–579 (2005).
5. Reynaud, E. G. *et al.* Human Lsg1 defines a family of essential GTPases that correlates with the evolution of compartmentalization. *BMC Biol* **3**, 21 (2005).
6. Kallstrom, G., Hedges, J. & Johnson, A. The putative GTPases Nog1p and Lsg1p are required for 60S ribosomal subunit biogenesis and are localized to the nucleus and cytoplasm, respectively. *Mol Cell Biol* **23**, 4344–4355 (2003).
7. Loewen, C. J. R., Roy, A. & Levine, T. P. A conserved ER targeting motif in three families of lipid binding proteins and in Opi1p binds VAP. *EMBO J* **22**, 2025–2035 (2003).
8. Kaiser, S. E. *et al.* Structural Basis of FFAT Motif-Mediated ER Targeting. *Structure* **13**, 1035–1045 (2005).
9. Oughtred, R. *et al.* The BioGRID database: A comprehensive biomedical resource of curated protein, genetic, and chemical interactions. *Protein Sci* **30**, 187–200 (2021).
10. Cho, K. F. *et al.* Split-TurboID enables contact-dependent proximity labeling in cells. *Proceedings of the National Academy of Sciences* **117**, 12143–12154 (2020).
11. Ni, C. *et al.* Labeling of heterochronic ribosomes reveals C1ORF109 and SPATA5 control a late step in human ribosome assembly. *Cell Reports* **38**, (2022).
12. Di Mattia, T. *et al.* FFAT motif phosphorylation controls formation and lipid transfer function of inter-organelle contacts. *EMBO J* **39**, e104369 (2020).
13. Sutjita, P. *et al.* The Ribosome Assembly Factor LSG1 Interacts with Vesicle-Associated Membrane Protein-Associated Proteins (VAPs). *Mol Cell Biol* **44**, 345–357 (2024).
14. Hornbeck, P. V. *et al.* PhosphoSitePlus: a comprehensive resource for investigating the structure and function of experimentally determined post-translational modifications in man and mouse. *Nucleic Acids Res* **40**, D261–D270 (2012).
15. Zhang, Z. *et al.* A subcellular map of translational machinery composition and regulation at the single-molecule level. *Science* **387**, eadn2623 (2025).
16. Yu, J. *et al.* Phosphorylation switches protein disulfide isomerase activity to maintain proteostasis and attenuate ER stress. *EMBO J* **39**, e103841 (2020).
17. Hardt, R. *et al.* Proteomic investigation of neural stem cell to oligodendrocyte precursor cell differentiation reveals phosphorylation-dependent Dclk1 processing. *Cell. Mol. Life Sci.* **80**, 260 (2023).

This preprint was submitted under the following conditions:

- The authors declare that the necessary Terms of Free and Informed Consent of participants or patients in the research were obtained and are described in the manuscript, when applicable.
- The authors declare that the preparation of the manuscript followed the ethical norms of scientific communication.
- The authors declare that they are aware that they are solely responsible for the content of the preprint and that the deposit in SciELO Preprints does not mean any commitment on the part of SciELO, except its preservation and dissemination.
- The authors declare that the data, applications, and other content underlying the manuscript are referenced.
- The deposited manuscript is in PDF format.
- The authors declare that the research that originated the manuscript followed good ethical practices and that the necessary approvals from research ethics committees, when applicable, are described in the manuscript.
- The authors declare that once a manuscript is posted on the SciELO Preprints server, it can only be taken down on request to the SciELO Preprints server Editorial Secretariat, who will post a retraction notice in its place.
- The authors agree that the approved manuscript will be made available under a Creative Commons CC-BY license.
- The submitting author declares that the contributions of all authors and conflict of interest statement are included explicitly and in specific sections of the manuscript.
- The authors declare that the manuscript was not deposited and/or previously made available on another preprint server or published by a journal.
- If the manuscript is being reviewed or being prepared for publishing but not yet published by a journal, the authors declare that they have received authorization from the journal to make this deposit.
- The submitting author declares that all authors of the manuscript agree with the submission to SciELO Preprints.